Multiphoton spectral microscopy for imaging and quantification of tissue glycation

Jo-Ya Tseng,[1] Ara A. Ghazaryan,[1] Wen Lo,[1,2] Yang-Fang Chen,[1] Vladimir Hovhannisyan,[1] Shean-Jen Chen,[2] Hsin-Yuan Tan,[3,4,7] and Chen-Yuan Dong[1,5,6,8]

[1]*Department of Physics, National Taiwan University, Taipei 106, Taiwan*
[2]*Department of Engineering Science, National Cheng Kung University, Tainan, Taiwan*
[3]*Department of Biomedical Engineering, National Taiwan University*
[4] *Department of Ophthalmology, Chang Gung Memorial Hospital; College of Medicine, Chang Gung University, Linko, Taiwan*
[5]*Center for Quantum Science and Engineering, National Taiwan University, Taipei 106, Taiwan*
[6] *Biomedical Molecular Imaging Core, Division of Genomic Medicine, Research Center for Medical Excellence, National Taiwan University, Taipei, Taiwan*
[7]*d93548010@ntu.edu.tw*
[8]*cydong@phys.ntu.edu.tw*

Abstract: Tissue glycation from diabetes and aging can result in complications such as renal failure, blindness, nerve damage and vascular diseases. In this work, we applied multiphoton microscopy for imaging and characterizing the extent of tissue glycation. The characteristic features of multiphoton autofluorescence (MPAF) and second harmonic generation (SHG) images as well as MPAF spectra of glycated bovine skin, cornea and aorta were acquired. The analysis of MPAF intensity change accompanying the glycation process shows that collagen is more responsive to the formation of autofluorescent advanced glycation endproducts (AGEs) than elastic fibers. Changes in spectral features were also used to estimate the rate of glycation in tissues with intrinsic AF. Our study shows that multiphton imaging may be used for the *in vitro* investigation of the effects of tissue glycation and that this approach may be used for monitoring AGE formation in the clinical setting.

OCIS codes: (120.3890) Medical optics instrumentation; (170.5810) Scanning microscopy; (170.6510) Spectroscopy, tissue diagnostics; (180.4315) Nonlinear microscopy.

References and links

1. N. Ahmed, "Advanced glycation endproducts--role in pathology of diabetic complications," Diabetes Res. Clin. Pract. **67**(1), 3–21 (2005).
2. M. Brownlee, "Biochemistry and molecular cell biology of diabetic complications," Nature **414**(6865), 813–820 (2001).
3. N. Verzijl, J. DeGroot, S. R. Thorpe, R. A. Bank, J. N. Shaw, T. J. Lyons, J. W. Bijlsma, F. P. Lafeber, J. W. Baynes, and J. M. TeKoppele, "Effect of collagen turnover on the accumulation of advanced glycation end products," J. Biol. Chem. **275**(50), 39027–39031 (2000).
4. T. J. Sims, L. M. Rasmussen, H. Oxlund, and A. J. Bailey, "The role of glycation cross-links in diabetic vascular stiffening," Diabetologia **39**(8), 946–951 (1996).
5. R. Meerwaldt, R. Graaff, P. H. N. Oomen, T. P. Links, J. J. Jager, N. L. Alderson, S. R. Thorpe, J. W. Baynes, R. O. B. Gans, and A. J. Smit, "Simple non-invasive assessment of advanced glycation endproduct accumulation," Diabetologia **47**(7), 1324–1330 (2004).
6. E. L. Hull, M. N. Ediger, A. H. T. Unione, E. K. Deemer, M. L. Stroman, and J. W. Baynes, "Noninvasive, optical detection of diabetes: model studies with porcine skin," Opt. Express **12**(19), 4496–4510 (2004).
7. L. Kessel, B. Sander, P. Dalgaard, and M. Larsen, "Lens fluorescence and metabolic control in type 1 diabetic patients: a 14 year follow up study," Br. J. Ophthalmol. **88**(9), 1169–1172 (2004).
8. H. J. Van Schaik, J. Coppens, T. J. Van den Berg, and J. A. Van Best, "Autofluorescence distribution along the corneal axis in diabetic and healthy humans," Exp. Eye Res. **69**(5), 505–510 (1999).
9. R. Gillies, G. Zonios, R. R. Anderson, and N. Kollias, "Fluorescence excitation spectroscopy provides information about human skin in vivo," J. Invest. Dermatol. **115**(4), 704–707 (2000).

#132618 - $15.00 USD Received 2 Aug 2010; revised 14 Nov 2010; accepted 17 Dec 2010; published 24 Dec 2010

10. J. Hadley, N. Malik, and K. Meek, "Collagen as a model system to investigate the use of aspirin as an inhibitor of protein glycation and crosslinking," Micron **32**(3), 307–315 (2001).
11. V. Hovhannisyan, W. Lo, C. Hu, S. J. Chen, and C. Y. Dong, "Dynamics of femtosecond laser photo-modification of collagen fibers," Opt. Express **16**(11), 7958–7968 (2008).
12. V. A. Hovhannisyan, P. J. Su, Y. F. Chen, and C. Y. Dong, "Image heterogeneity correction in large-area, three-dimensional multiphoton microscopy," Opt. Express **16**(7), 5107–5117 (2008).
13. B. M. Kim, J. Eichler, K. M. Reiser, A. M. Rubenchik, and L. B. Da Silva, "Collagen structure and nonlinear susceptibility: effects of heat, glycation, and enzymatic cleavage on second harmonic signal intensity," Lasers Surg. Med. **27**(4), 329–335 (2000).
14. V. M. Monnier, R. R. Kohn, and A. Cerami, "Accelerated age-related browning of human collagen in diabetes mellitus," Proc. Natl. Acad. Sci. U.S.A. **81**(2), 583–587 (1984).

1. Introduction

Protein glycation is initiated by spontaneous non-enzymatic reactions between free amino groups on long lived proteins and carbonyl groups of reducing sugars to form a chemically reversible Schiff base adducts which are further rearranged in becoming the more stable Amadori product. Subsequently, a number of reactions result in the formation of poorly characterized structures known as AGEs [1] some of which act as crosslinking agents within and between protein molecules [2]. The glycation process and formation of crosslinks are thought to contribute to many of the complications seen in aging and diabetes mellitus. The extent of tissue glycation depends on the degree of hyperglycaemia, half-life of the protein, availability of free amino groups for reaction, and permeability of the tissue to free sugar molecules.

Due to their long half-life, the level of AGEs in collagen acts as a long-term integrator of overall glycemia that is insensitive to short- or intermediate-term fluctuations in glycemic control [3]. Consequently, AGEs accumulate naturally during healthy aging, but at significantly accelerated rates in persons with diabetes. Increased glycation and, in particular, accumulation within tissue and serum of AGEs have an important role in the pathogenesis of diabetic complications [1,2]. To be specific, the AGE-mediated crosslinking of collagen and consequent alterations of structural-mechanical changes in the vascular system is one of the causes responsible for development and expression of atherosclerosis and its complications such as diabetic vascular stiffening [4]. AGEs can be assayed by invasive procedures requiring a biopsy specimen. However, such procedures cannot be used for the frequent screening and diagnosis of disease progression in diabetic patients. An accurate, convenient, and noninvasive screening test would be an attractive alternative to current methodologies.

Recent studies have shown that noninvasive optical spectroscopy offers one approach for the noninvasive detection of tissue glycation by measuring autofluorescent AGEs in tissues such as skin and cornea [5–8]. These studies demonstrate the feasibility of using spectral detection of autofluorescence in assessing the degree of tissue glycation in diabetic patients. The current techniques of detecting the formation of autofluorescent AGE species use one-photon excited autofluorescence from AGE species such as crossline and pentosidine [5,6,9]. However, without additional visualization aid, it is not possible to separate the contribution of autofluorescence from other tissue components such as elastic fibers or cells. Moreover, spectral measurements cannot distinguish the effect of glycation on different tissue components such as collagen and elastic fibers. Therefore, in the present study, we propose to use multiphoton microscopy to demonstrate the feasibility of using multiphoton imaging for visualizing and evaluation of glycated tissues and to investigate the effect of glycation on collagen and elastic fibers, two of the most important connective tissues in mammals. With the known advantages of multiphoton microscopy such as deeper tissue penetration, higher special resolution, reduced photodamage, and resolution of second harmonic generating collagen fibers, diagnosis of tissue glycation may be improved.

In this study, we performed multiphoton spectral imaging on bovine cornea, skin, and aorta tissues treated with ribose solution to induce glycation. Specifically, multiphoton

#132618 - $15.00 USD Received 2 Aug 2010; revised 14 Nov 2010; accepted 17 Dec 2010; published 24 Dec 2010

autofluorescence (MPAF) and second harmonic generation (SHG) from these specimens were gathered for image analysis.

1.1. Materials and method

Glycated tissue samples preparation

Three different tissue types of bovine origin that are rich in connective fibers were used in this study: cornea, skin, and aorta. All samples were obtained from local markets and processed in order to expose the connective tissues intended for our glycation study. Freshly obtained corneas were excised from intact eyeballs into button shape 7 mm in diameter. Bovine skin was scraped with blades to remove fur and epidermis to expose collagen-rich dermal layer. To obtain images of both inner and outer walls of the aorta, thin cross-sectional slices 3-4 mm in size were cut from fresh vessels using scalpels. Prior to incubation all samples were cut into small sections of equal sizes (approximately $2 \times 4 \times 15$ mm^3), thoroughly washed in phosphate buffered saline (PBS) solution, soaked in 1% povidone-iodine solution for about 10 seconds and washed in PBS.

Tissue glycation was induced by incubating the tissue in 0.5M ribose solution to mimic physiological hyperglycemia. The composition of solutions was obtained from a previous work and slightly altered for our needs [10]. One section of each tissue was incubated in 10 ml of control solution and 3 samples were incubated in the glycation solution composed of 0.05 M PBS (Sigma-Aldrich, St. Louis, MO), 1% penicillin-streptomycin and 5% dextran T500 (Pharmacosmos, Holbaek, Denmark) containing 0.5 M ribose (Sigma, R9629-100G). The solution used for the control group tissues had the same chemical composition as the glycation solution with ribose excluded. All tissues were incubated at 37°C and 5% of CO_2 condition for different periods of 2, 4, 6, 8, 10 days. Untreated tissue was considered as Day 0 specimen both for glycated and control specimens. At the end of the incubation period, the samples were rinsed with PBS buffer to remove the excess ribose. Vessel and skin samples were dissected into smaller pieces (approximately $1 \times 2 \times 4$ mm^3) while the button-shape of cornea samples was retained. All samples were sealed within a microscope slide and No. 1.5 coverglass for imaging purposes.

Multi-photon microscopy

The multiphoton microscope used in this study is similar to one described previously [11]. In brief, MPAF and SHG images were obtained using laser scanning microscope system (LSM 510 META, Zeiss, Jena, Germany) coupled to a fs, titanium:sapphire (ti:sa) laser (Tsunami, Spectra-Physics, Mountain View, CA). A water immersion objective (Zeiss, C-Apochromat 40 × /NA 1.2, WD = 0.28 mm) was used for focusing the laser source and collection of the emission signal in the epi-illuminated geometry. To explore the multiphoton excitation properties of the glycated tissues, excitation wavelengths in the range 720 – 800 nm in steps of 20 nm were used. The laser pulse width was estimated to be 100 fs with 80 MHz pulse repetition frequency. The average power of laser beam at the sample surface was 30 mW for the cornea specimens and 25 mW for skin and vessel tissues. These power limits were optimized for acquiring high image contrast while avoiding photobleaching. The images were acquired at the depths of approximately 50, 10 and 5 μm from the surfaces of cornea, skin and vessel samples respectively. All acquired optical images were 230×230 μm^2 in area with resolution of 512 x 512 pixels and pixel dwell time of 6.4 μs.

To visualize tissue glycation on a large scale, a specimen translation stage was used to translate the specimen after the acquisition of each small area optical image. In this manner, 9 adjacent images (3×3) were acquired and assembled into a larger-area image 690×690 μm^2 in size [12]. For broad band multiphoton imaging, the luminescence signals were acquired using the nondescanned detection (NDD) in which the MPAF and SHG signals were reflected

#132618 - $15.00 USD Received 2 Aug 2010; revised 14 Nov 2010; accepted 17 Dec 2010; published 24 Dec 2010

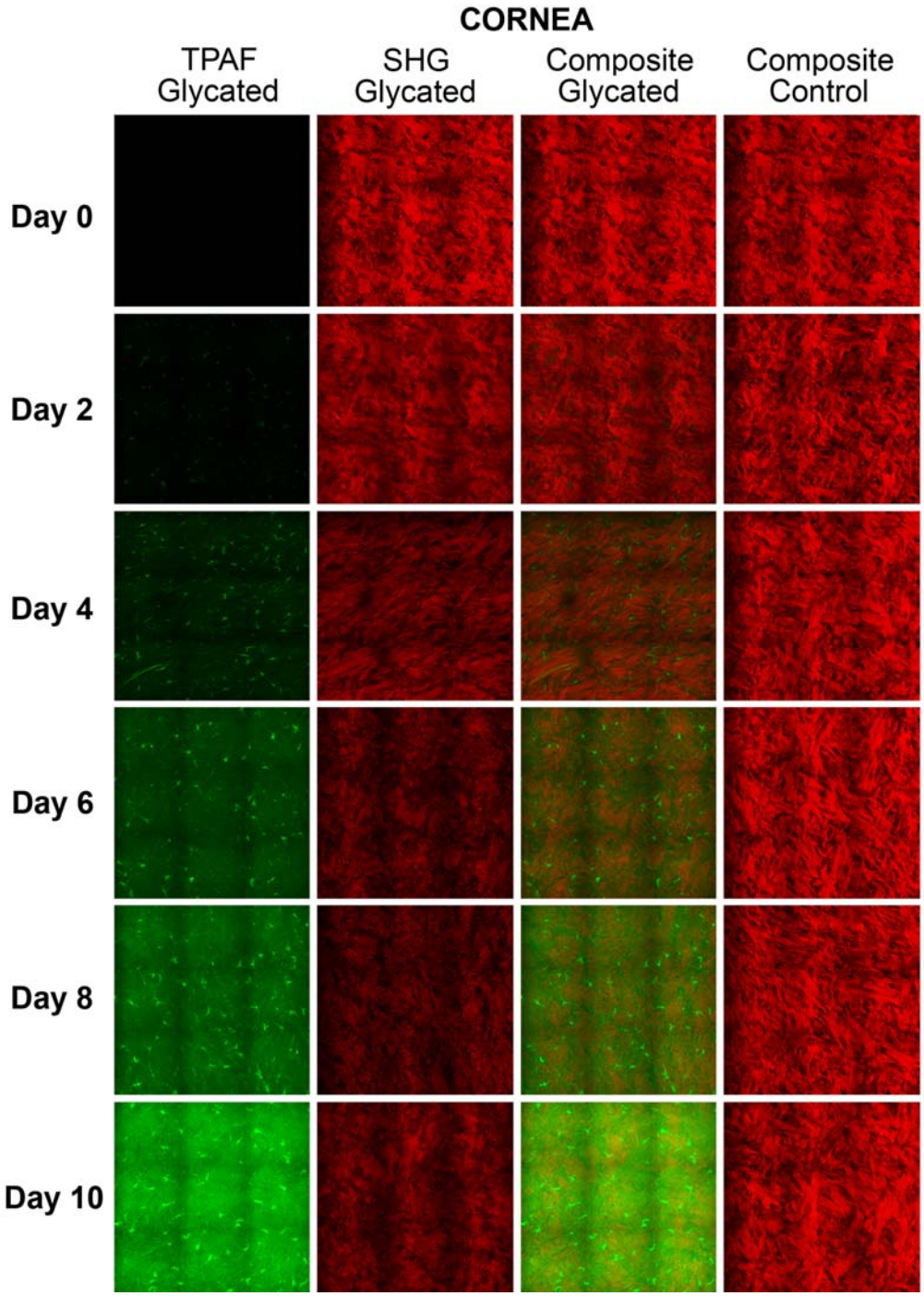

Fig. 1. Time course MPAF (green) and SHG (red) images of glycated and non-glycated samples of bovine cornea. The images of non-glycated control tissues are also shown for comparison. The laser excitation wavelength was 780 nm and the power was 180 mW. Frame size is 620 × 620 μm^2.

#132618 - $15.00 USD Received 2 Aug 2010; revised 14 Nov 2010; accepted 17 Dec 2010; published 24 Dec 2010

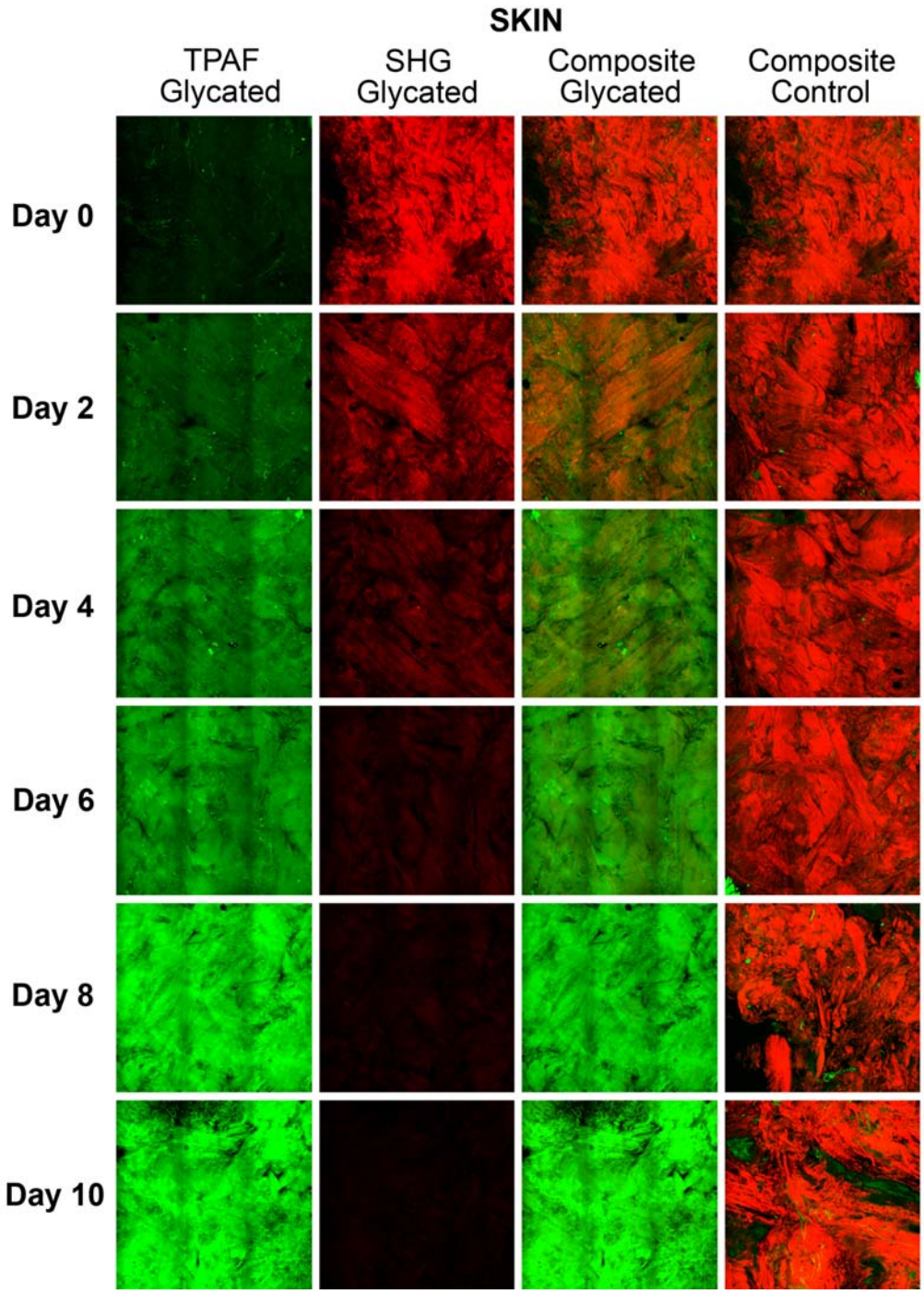

Fig. 2. Time course MPAF (green) and SHG (red) images of glycated and non-glycated samples of bovine skin. The images of non-glycated control tissues are also shown for comparison. The laser excitation wavelength was 780 nm and the power was 150 mW. Frame size is 620 × 620 μm^2.

#132618 - $15.00 USD Received 2 Aug 2010; revised 14 Nov 2010; accepted 17 Dec 2010; published 24 Dec 2010

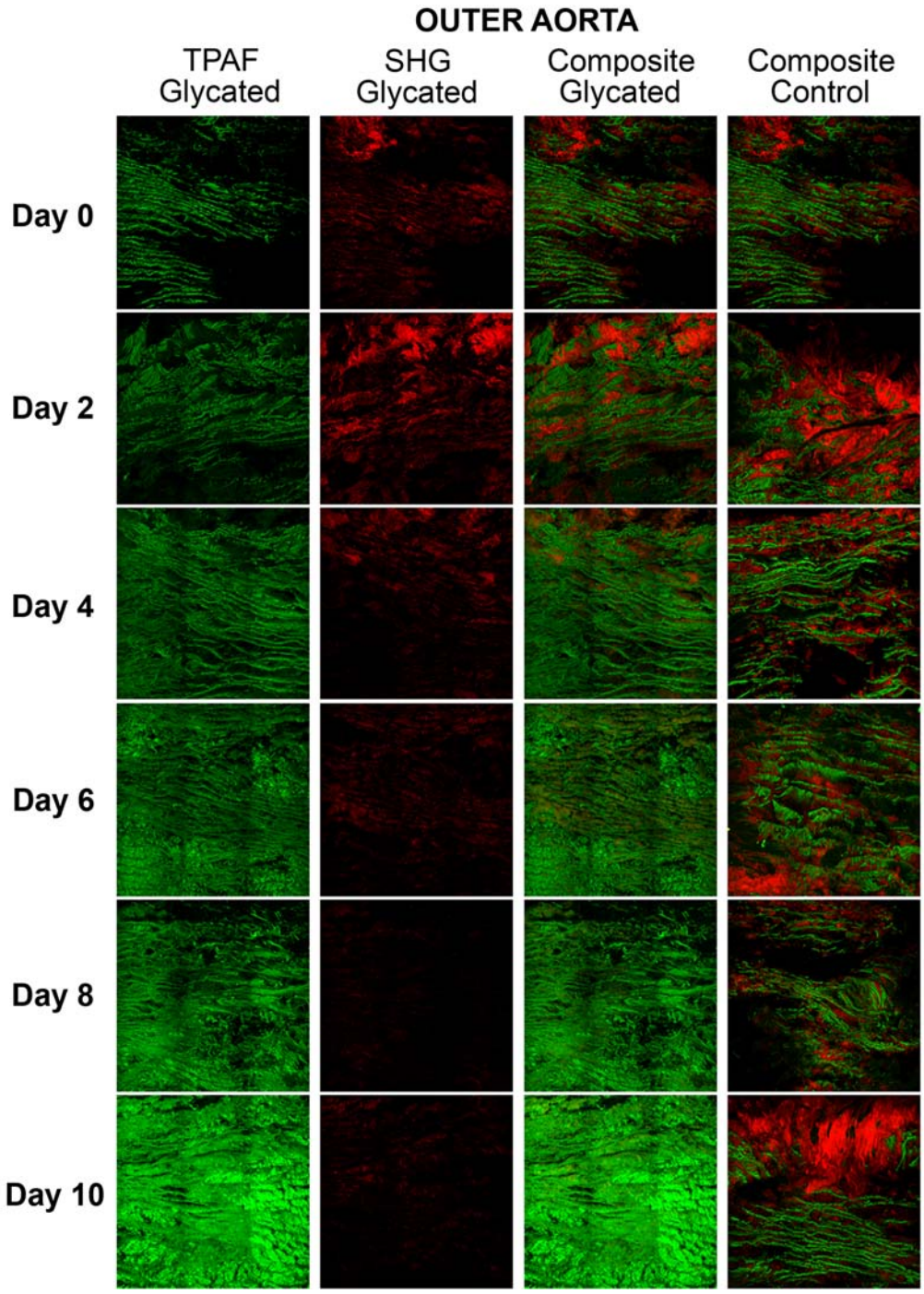

Fig. 3. Time course MPAF (green) and SHG (red) images of glycated and non-glycated specimens of outer aorta. The images of non-glycated control tissues are also shown for comparison. The laser excitation wavelength was 780 nm and the power was 180 mW. Frame size is 690 × 690 μm^2.

#132618 - $15.00 USD Received 2 Aug 2010; revised 14 Nov 2010; accepted 17 Dec 2010; published 24 Dec 2010

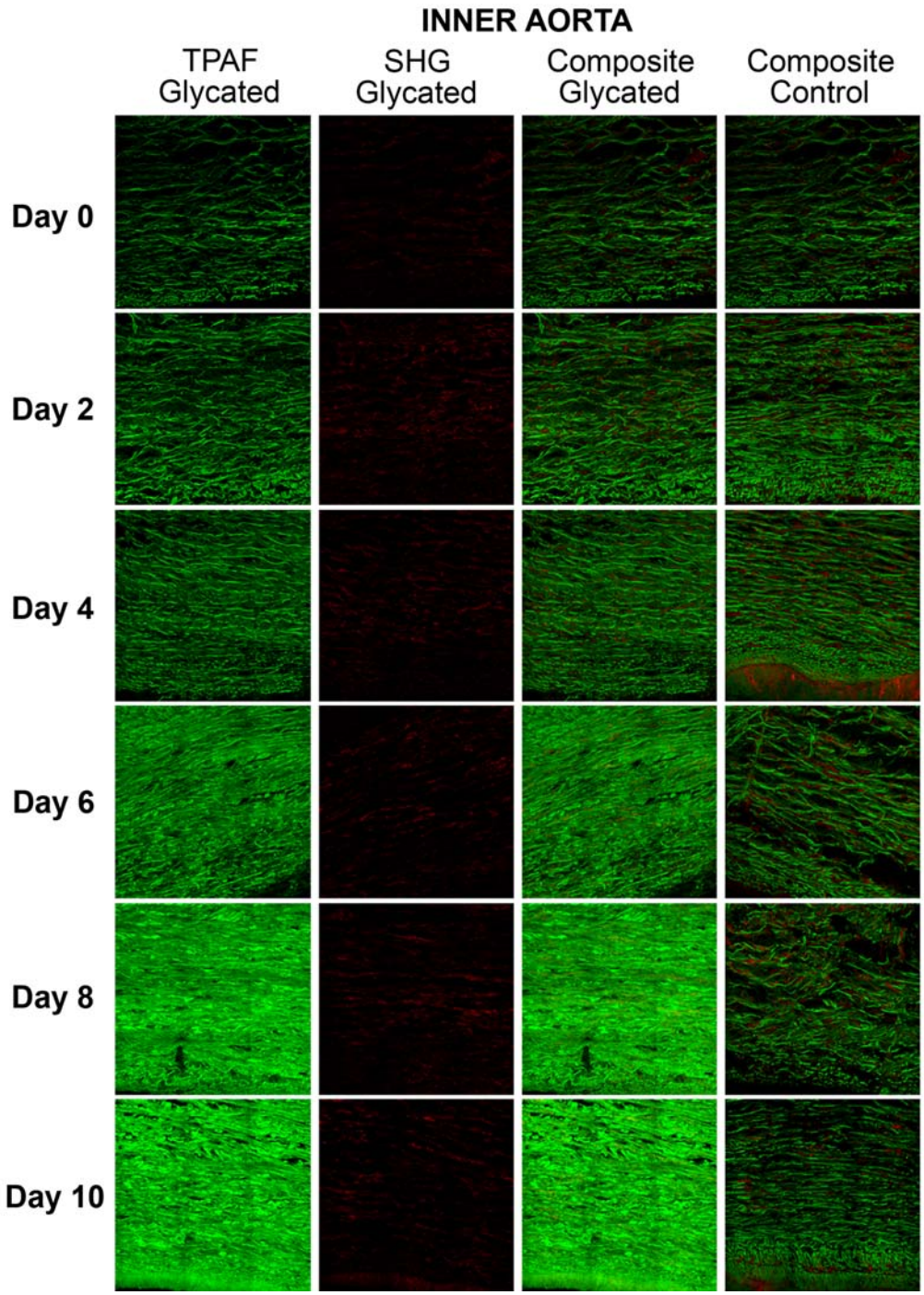

Fig. 4. Time course MPAF (green), SHG (red) images of glycated and non-glycated specimens of inner aorta. The images of non-glycated control tissues are also shown for comparison. The laser excitation wavelength was 780 nm and the power was 180 mW. Frame size is 690 × 690 μm^2.

#132618 - $15.00 USD Received 2 Aug 2010; revised 14 Nov 2010; accepted 17 Dec 2010; published 24 Dec 2010

by the dichroic mirror (NDD LP 680) and further separated by the combination of a secondary dichroic mirror (FT 440) and two bandpass filters for the detection of broadband MPAF (435-700 nm) and SHG (380-400 nm). For spectral imaging, the signal was detected in the descanned mode where the reflected excitation beam and specimen luminescence was descanned and reflected from a dichroic mirror (HFT KP650) into a grating for 16 channel spectral imaging in the 377-720 nm range with a 21.4 nm detection bandwidth. All imaging experiments were conducted at the ambient temperature of 19° C.

1.2. Data collection and analysis

Prior to analysis and presentation of the large area images (3 × 3 tiles), the images were processed with a lateral image heterogeneity correction algorithm. This approach (applied to Figs. 1-4) allowed correcting for differences in excitation and collection efficiency within each small area image [12]. For quantitative analysis of the spectral data, we selected 5 regions of interests (ROIs) to compute the average MPAF and SHG intensities. To test differences in the glycation rate between collagen and elastic fibers, 5 ROIs (each 70 μm in diameter) within the tissue specimens containing either collagen or elastic fibers were selected for analysis. The discrimination between the two fiber types was made based on the appearance of SHG signal, which was present in collagen but not elastic fibers. At every time point, quantitative image analysis was performed.

2. Results and discussion

2.1 MPAF and SHG images

Time course changes in MPAF and SHG of glycated bovine cornea and skin are shown in Fig. 1 and Fig. 2 respectively. The images of non-glycated (control) tissues are also shown. Qualitatively, it is clear that glycation resulted in drastic increase of MPAF intensity and moderate decrease in SHG.

In addition, the images we acquired of outer and inner aorta are shown in Fig. 3 and Fig. 4 respectively. Since the outer aorta consists of both collagen and elastic fibers while the inner aorta is composed primarily of elastic fibers, imaging the two locations within the aorta would enable us to determine the effects of glycation on different types of connective tissues. As Fig. 3 and Fig. 4 show, both collagen and elastic fibers are susceptible to glycation as autofluorescence increased for both outer and inner aorta.

2.2 Quantification of tissue glycation using MPAF and SHG intensities

From the time-course images of cornea, skin and aorta specimens, the average intensities of MPAF and SHG as a function of time were computed. Shown in Fig. 5A, B, C, and D are the results for cornea, skin, outer aorta, and inner aorta respectively. Each data point represents the average of 15 ROIs from the specimens. The images used for intensity analysis were obtained using excitation wavelength of 780 nm.

As can be clearly seen from Fig. 5, all four specimens showed similar trends for MPAF intensity. During the first 2 days the intensity of collagen-rich tissue shows moderate increase. However, starting from Day 2, MPAF dramatically increased in a linear fashion. During the 10-day glycation period, MPAF increased by factors of: 54.5 ± 4.0 in cornea, 17.5 ± 2.3 in skin dermal collagen, 1.42 ± 0.3 in elastin of inner aorta, 2.26 ± 0.4 in elastin from outer aorta, and 24.9 ± 8.4 in collagen from outer aorta. In contrast, the AF intensity of control group remained the same within experimental error for all treatment times. The intensity of the SHG signal decreased in glycated cornea and skin. In contrast, no statistically significant change of SHG was observed in the control samples. This observation is consistent with previous reports and indicates glycation-induced disorder in the collagen structure [13]. In comparison, the SHG intensity change of aorta does not show a general tendency but

#132618 - $15.00 USD Received 2 Aug 2010; revised 14 Nov 2010; accepted 17 Dec 2010; published 24 Dec 2010

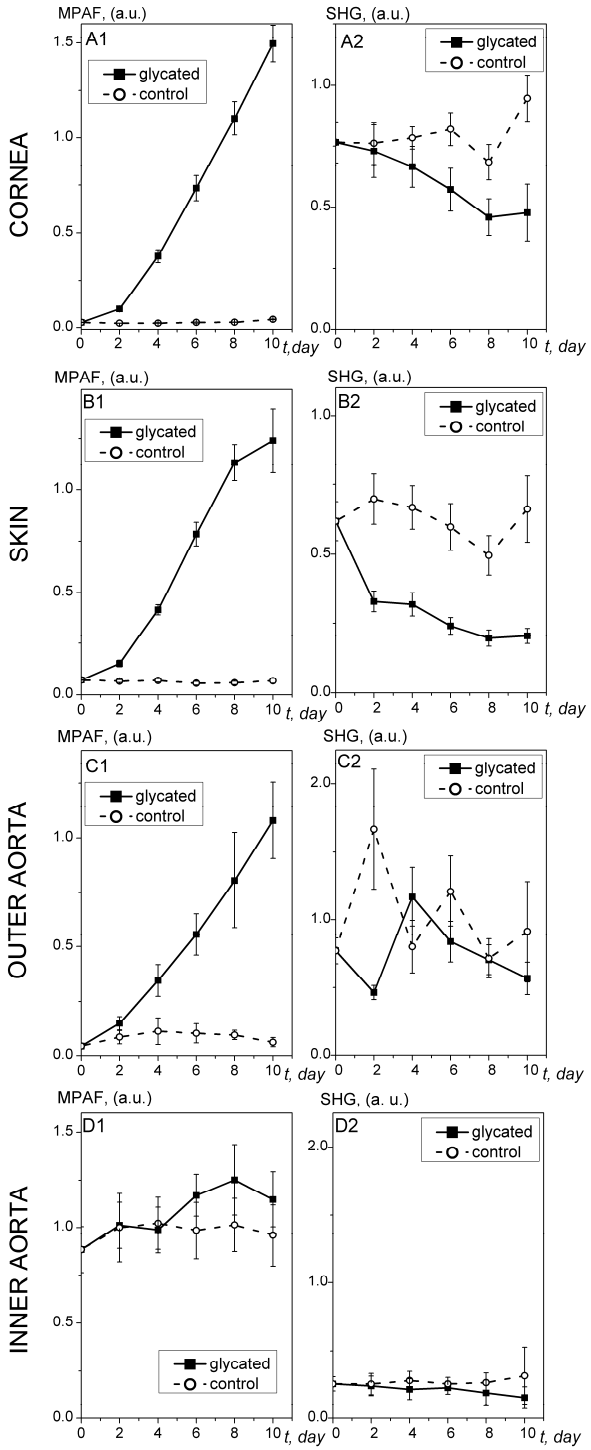

Fig. 5. The dependence of MPAF (left panels) and SHG (right panels) signal intensity of cornea (A), skin (B), outer aorta (C),and inner aorta (D) on the incubation time in 0.5 M ribose (glycated) or PBS (control). Each data point is an average of 15-16 ROIs.

#132618 - $15.00 USD Received 2 Aug 2010; revised 14 Nov 2010; accepted 17 Dec 2010; published 24 Dec 2010

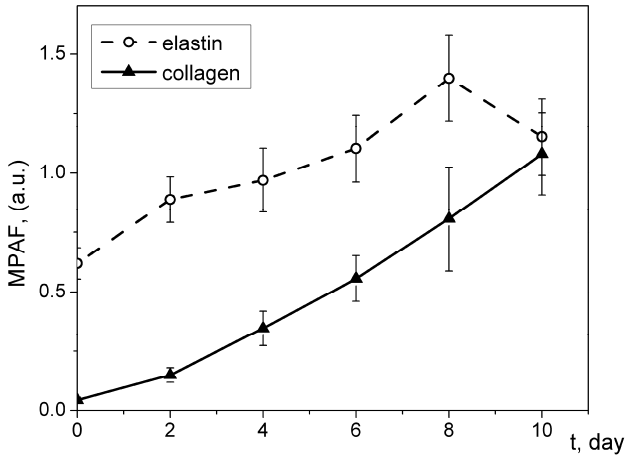

Fig. 6. Relative change of elastin and collagen MPAF intensity from aorta. 30 ROIs of elastic fibers where selected from both outer and inner part of aorta. For collagen, 15 ROIs from outer aorta were analyzed. The excitation wavelength used for image acquisition was 780 nm and the laser power was 150 mW.

fluctuates with time (Fig. 5, C2). Despite the fact that the presence of SHG can serve as a footprint of collagen containing tissue, it is the MPAF rather than SHG signal that is a more sensitive metric for the quantitative determination of the extent of tissue glycation.

In an attempt to compare the relative glycation rates of collagen and elastic fibers, the temporal dependence of MPAF intensity was obtained by analyzing signal change at specific sites of outer aorta. Figure 6 represents the relative change of MPAF intensity at elastin- and collagen-rich sites of aorta. The elastin MPAF increased by a factor of 2.26 ± 0.4 on Day 8 whereas for collagen the MPAF increased 24.9 ± 8.4 times (Day 10).

Our results show that collagen is more responsive to the formation of autofluorescent AGEs than elastic fibers and indicate that its relatively low intrinsic autofluorescence enables collagen to be used for a reliable and accurate determination of tissue glycation.

2.3 Spectral analysis

In addition to broadband MPAF analysis, we also employed the lambda mode of the Zeiss 510 system to measure the MPAF spectral data of all tissues under study at different excitation wavelengths of 720, 740, 760, 780 and 800 nm. The images were obtained for samples of bovine cornea, skin and aorta treated for 10 days in PBS and ribose solution. The spectra of cornea, skin, outer aorta, and inner aorta treated for 10 days are respectively shown in Fig. 7(A), (B), (C), and (D) along with the control data. The shape of spectra obtained from skin are similar to the ones obtained previously using one-photon excitation of 370-400 nm [14]. For all glycated tissues, the position of maxima of spectra is around 495 nm under the excitation wavelengths used. However, in the case of outer aorta, the spectra of glycated and control specimens are distinctively different. For outer aorta, we observed another feature of spectral change and it is the shift of the spectral maximum from about 473 to approximately 495 nm. This effect is most pronounced for the spectra of control samples and Day 10 glycated specimens obtained under the excitation of 720 nm and is most likely due to the shift of MPAF maxima for elastin in tissue. Specifically, the MPAF maxima are around 473 nm under 720 nm excitation and are distinguishable from the spectra of glycated samples with maxima at 495 nm. To evaluate the effectiveness of using spectral shift as a measure of glycation, we have normalized time course spectra of both glycated and non-glycated tissues obtained using 720 nm excitation (Fig. 8).

#132618 - $15.00 USD Received 2 Aug 2010; revised 14 Nov 2010; accepted 17 Dec 2010; published 24 Dec 2010

The arrows show the tendency of spectrum shift during the course of treatment in ribose solution. The difference between the Day 10 and Day 0 is presented with dashed line. Obviously, the shift and perturbations of the shape of spectra are negligible for the control tissues (Fig. 8(A) and Fig. 8(C)). However, the spectra of glycated aorta are red shifted under 720 nm excitation. This effect is more pronounced for outer aorta (Fig. 8(D)).

The comparison of spectrum obtained from elastin rich inner part of aorta with the ones obtained for collagen-rich sites of outer aorta brings additional information about the origin of the observed shift (Fig. 9).

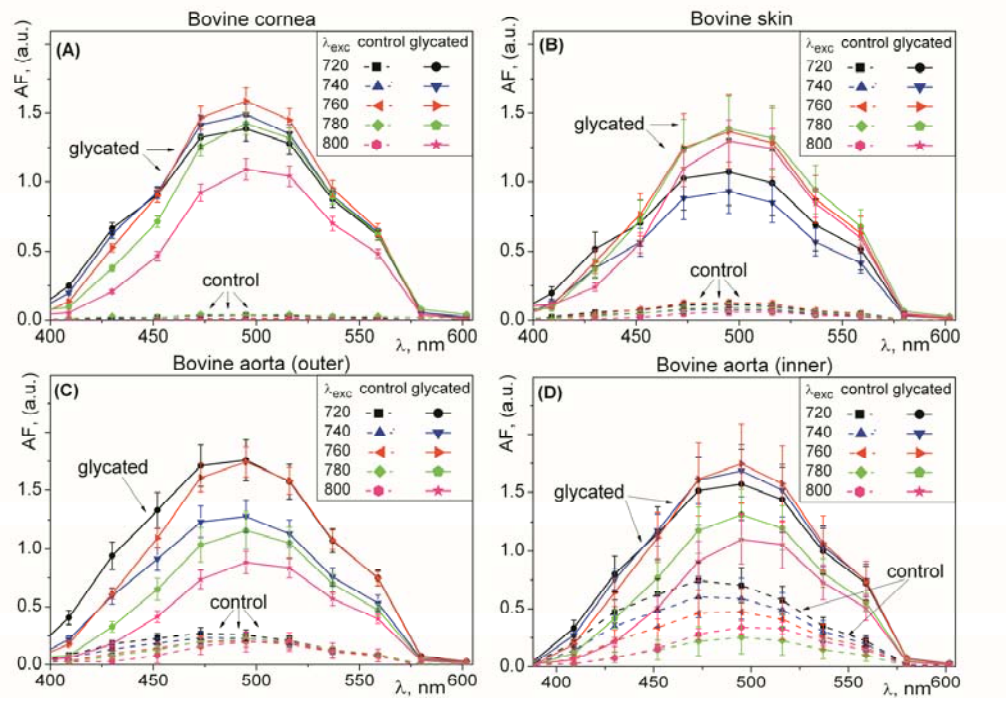

Fig. 7. MPAF spectra of glycated (solid lines) and non-glycated (dashed lines) cornea (A), skin (B), outer (C) and inner (D) aorta obtained using the excitations wavelengths of 720, 740, 760, 780, and 800 nm.

Clearly, the maxima of both glycated elastin and collagen spectra are around 495 nm, whereas the spectral maximum of non-glycated elastin is 473 nm. The fact that the shift is evident for elastin explains why similar shift was not found for cornea and skin, where elastin is absent or less abundant. This also explains why the spectral shift is more pronounced in outer part of the vessel where both elastin and collagen are present. Despite these observations it should be noted that the spectral change is not as sensitive as the change in MPAF intensity in detecting tissue glycation. Therefore, MPAF intensity change of collagen, rather than spectral shift measurements, should be used as the detection mechanism of tissue glycation.

#132618 - $15.00 USD Received 2 Aug 2010; revised 14 Nov 2010; accepted 17 Dec 2010; published 24 Dec 2010

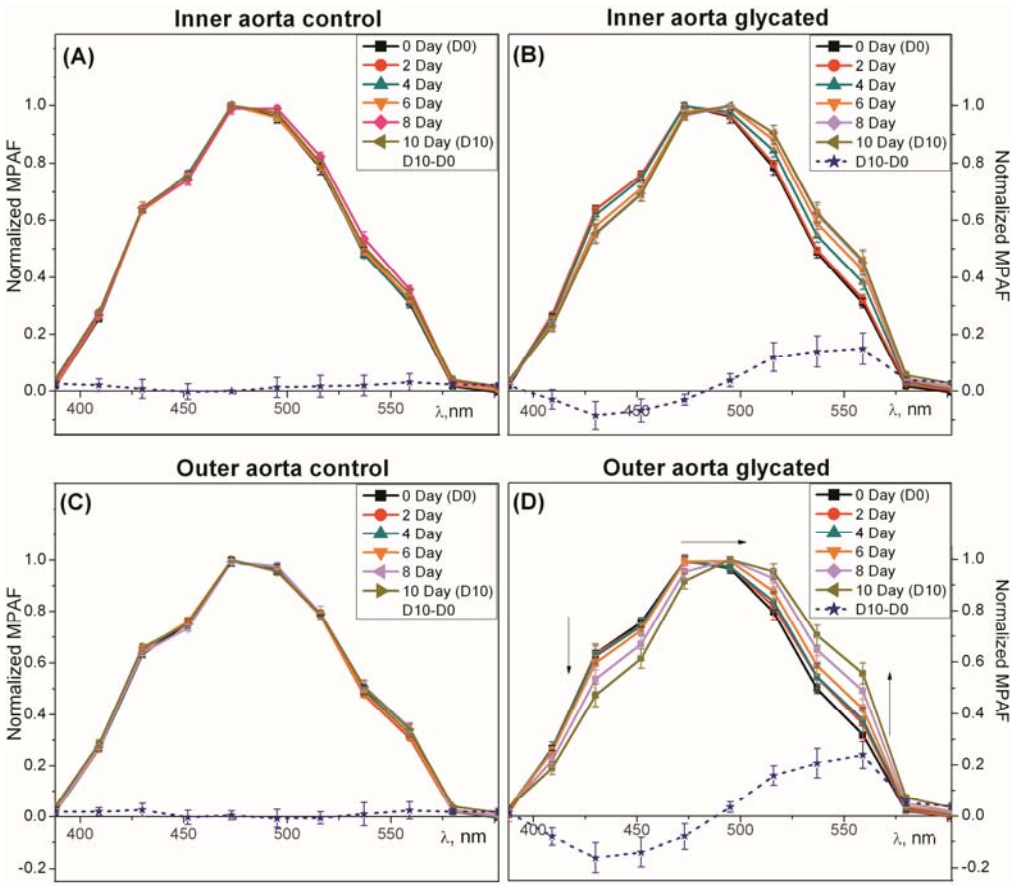

Fig. 8. Changes of normalized MPAF spectra of inner (upper panels) and outer (lower panels) aorta during the treatment with PBS (control: left panels) and 0.5 M ribose (glycated: right panels). The spectra were obtained using λ_{exc} = 720 nm. The difference of spectra at Day 10 and Day 0 is also shown (dashed lines). The arrows in (D) indicate the time course of glycation.

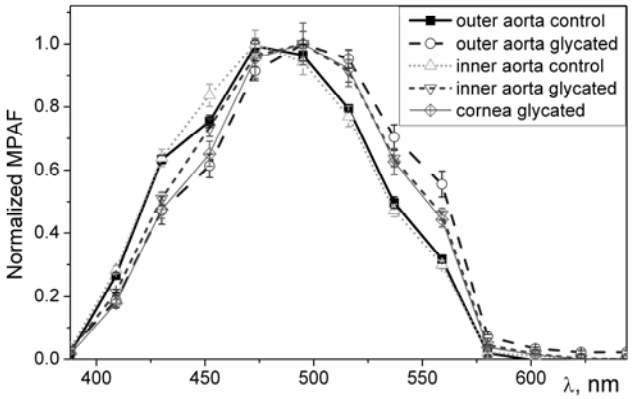

Fig. 9. Normalized MPAF spectra of both glycated and non-glycated inner and outer aorta and glycated cornea. Spectra were obtained using excitation wavelengths of 720 nm.

#132618 - $15.00 USD Received 2 Aug 2010; revised 14 Nov 2010; accepted 17 Dec 2010; published 24 Dec 2010

3. Conclusion

Multiphoton microscopy has a number of distinct advantages over the conventional methods for the non-invasive optical detection of AGEs. The analysis of two-photon AF intensity change accompanying the glycation process shows that collagen is more responsive to the formation of autofluorescent AGE products than elastic fibers. Changes in spectral features can also be used to monitor the rate of glycation in tissues with intrinsic AF. Our study shows that multiphoton imaging is capable of providing qualitative and quantitative information of the extent of tissue glycation. Provided the correlation between the and conventional parameters for degree of glycation (such as HbA1C) and developed non-invasive imaging analysis, this approach has potential for monitoring AGE formation in the clinical setting and can be applied in both *in vivo* and *in vitro* studies aiming at understanding the effect of glycation on physiological disorders.

Acknowledgments

Authors Jo-Ya Tseng and Ara A. Ghazaryan contributed equally to this work. This study was financially supported by the National Science Council, Taiwan (NSC – 98-2112-M-002-008-MY3), NTU (NTU-99R70409) and Center for Quantum Science and Engineering (CQSE-99R80870).

#132618 - $15.00 USD Received 2 Aug 2010; revised 14 Nov 2010; accepted 17 Dec 2010; published 24 Dec 2010